Organelle targeting of myosin XI is mediated by two globular tail subdomains with separate cargo binding sites

Jian-Feng Li and Andreas Nebenführ

Supporting Information

RESULTS

Application of Swiss-modeling to Myo2p—The published high-resolution three-dimensional structure for Myo2p globular tail is missing some interior small segments, presumably due to spatial disorder or proteolytic instability (1). We set up a test for the efficiency of Swiss-Model methodology (2) by using the complete globular tail sequence of Myo2p as a query and then comparing the computational result with the known structure. The missing parts in the crystal structure turned out in the predicted structure to be spatially flexible loops with the exception of a short putative α-helix between H6 and H7 (purple segments in Fig. 1*B*). The remainder of the predicted Myo2p tail structure matched the experimentally determined structure perfectly (RMS deviation 0.15Å), suggesting Swiss-Model is a proficient tool for tertiary structure prediction.

Ramachandran plot of the structure model of MYA1 globular tail—The stereochemical quality of our structure model of MYA1 globular tail was assessed by Ramachandran plot (3). A good-quality structure model is expected to have more than 95% of all non-glycine residues lying in the energetically allowed regions in a Ramachandran map (4). In our case, only 10 non-glycine residues (less than 2.5%) scattered over the energetically unfavorable area in the Ramachandran map (Supplemental Fig. 1*A*). All these residues were present in loop regions of the predicted structure where folding predictions are notoriously difficult. Thus, we concluded that the structure model is sterically reliable.

RMSD calculation of individual amino acid residues in MYA1-Myo2p alignment—The quality of fit for a given amino acid sequence can be calculated as the root-mean-square deviation (RMSD) of the predicted structure from the template structure. The overall RMSD value (1.91 Å) gives an indication how well the chain can fold into the template structure. However, a detailed analysis of the deviation of individual amino acids from their corresponding (i.e., aligned) template residues can reveal specific problems with the predicted structure. Supplemental Figure 1*B* reveals that the places with RMSD values > 1Å are all outside helical regions and typically flank gaps in the alignment, i.e. insertions or deletions in MYA1 relative to Myo2p. The largest deviations of the MYA1 chain from the Myo2p template are found between helices H2 and H3 and between H13 and H14 where MYA1 contains much shorter loop regions. These regions are difficult to predict and represent only an approximation of a likely structure for MYA1. However, the very low RMSD values within the helical regions (average 0.21 Å) suggest that the MYA1 sequence can take on the structure suggested by the Myo2p template. Four proline residues that reside within or near the end of predicted helices (P1093 in H1, P1123 in H3, P1245 and P1274 in H6) may result in slight distortions in the helical regions but apparently do not cause major disruptions of the

structure. Their Phi and Psi angles also fell into the energetically favorable region of the Ramachandran plot (Supplementary Figure 1*A*).

REFERENCES

1. Pashkova, N., Jin, Y., Ramaswamy, S., and Weisman, L.S. (2006) *EMBO J.* **25,** 693-700
2. Schwede, T., Kopp, J., Guex, N., and Peitsch, M.C. (2003) *Nucleic Acids Res*. **31,** 3381-3385
3. Ramachandran, G.N., Ramakrishnan, C., and Sasisekharan, V. (1963) *J. Mol. Biol.* **7,** 95-99
4. Chen, Y.W. (1994) *J. Appl. Cryst.* **27,** 660-661

Table S1: Summary of the primers used in this study

No.	Original name	Sequence	RS
P1	MYA1Y2HGT1-F	5' CGACTCGAGGACAGAAACAGCAGGAAAATCAA 3'	XhoI
P2	MYA1Y2HGT1-R	5' CGACTCGAGTCAATTATTTTGTGTATTTTGTG 3'	XhoI
P3	MYA1Y2HGT2-F	5' CGACCATGGGACCAAGGACACCGCGGTCTGG 3'	NcoI
P4	MYA1Y2HGT2-R	5' GCAGTCGACCTTCAATCTGACCTTTCCAACA 3'	SalI
P5	MYA2Y2HGT1-F	5' CTCGAGGAGAACGTCAAATTATGAATGTT 3'	XhoI
P6	MYA2Y2HGT1-R	5' CTCGAGTCAAGAATCTTTTCCAAAGGACCT 3'	XhoI
P7	MYA2Y2HGT2-F	5' CGACCATGGGACCCAGATCTTCTAAAGGAGG 3'	NcoI
P8	MYA2Y2HGT2-R	5' GCAGTCGACAACAATCACAGAGGAAGAGAGC 3'	SalI
P9	XIKY2HGT1-F	5' CGAGGATCCAGAAAAGCAACAGGAAAACCAG 3'	BamHI
P10	XIKY2HGT1-R	5' CGAGGATCCTCAAGCAACAGCATTTGCTTGTGC 3'	BamHI
P11	XIKY2HGT2-F	5' CGACCATGGGACCAAGGACATCAAGGGCAAG 3'	NcoI
P12	XIKY2HGT2-R	5' GCAGTCGACCGAGGGCAGTTACGATGTAC 3'	SalI
P13	XICY2HGT1-F	5' CTCGAGGAGAGAAGCAGCAAGAAAATCAA 3'	XhoI
P14	XICY2HGT1-R	5' CTCGAGTCAAGTGTTGCCAACGGAACGAGA 3'	XhoI
P15	XICY2HGT2-F	5' CGACCATGGGACCAAGAACATCGAGGGCTAG 3'	NcoI
P16	XICY2HGT2-R	5' GCAGTCGACAGAATCACTCAGAGACTGGC 3'	SalI
P17	MYA1Y2HGT-F	5' CGACCATGGGACAGAAACAGCAGGAAAATCAA 3'	NcoI
P18	MYA1GT1Δ1-R	5' CTCGAGTCACATTCCATATATCTTTTCTAG 3'	XhoI
P19	MYA1GT1Δ2-R	5' CTCGAGTCAGCAAGAAGCAAGCAGAGGGGA 3'	XhoI
P20	MYA1GT1Δ3-F	5' CTCGAGGATCTTTTGAAGTAGAAAGAACC 3'	XhoI
P21	MYA1GT1Δ4-F	5' CTCGAGGAAATCAAGAGCTGTTACTAAAA 3'	XhoI
P22	MYA1GT2Δ1-R	5' GCAGTCGACTCAGCTCTTTGATACATCTGACAC 3'	SalI
P23	MYA1GT2Δ2-R	5' GCAGTCGACTCAAAGCGAGAATGGGATGCTCGA 3'	SalI
P24	MYA1GT2Δ3-R	5' GCAGTCGACTCAGTTTTGGCGGATCAACGGAGG 3'	SalI
P25	MYA1GT2Δ4-R	5' GCAGTCGACTCACATGAAGTTGGAGTTTTGGCG 3'	SalI
P26	MYA1GT2Δ5-R	5' GCAGTCGACTCATTCCAACAAGAACATGAAGTT 3'	SalI
P27	YNXbaI-F	5' CGATCTAGAATGGTGAGCAAGGGCGAGGAG 3'	XbaI
P28	YNBamHI-R	5' CGAGGATCCCATGATATAGACGTTGTGGCT 3'	BamHI
P29	YCBamHI-F	5' CGAGGATCCGCCGACAAGCAGAAGAACGGC 3'	BamHI
P30	YCNotI-R	5' CGAGCGGCCGCTCAGTACAGCTCGTCCATGCCGAG 3'	NotI
P31	MYA1GT2BamHI-F	5' CGAGGATCC*GGTGGCCATCACCATCACCATCACGGTGGC*CCAA GGACACCGCGGTCTGGT 3'	BamHI
P32	MYA1GT2NotI-R	5' CGAGCGGCCGCTCAATCTGACCTTTCCAACAAGAA 3'	NotI
P33	MYA1GT1XbaI-F	5' CGATCTAGAATGCAGAAACAGCAGGAAAATCAA 3'	XbaI
P34	MYA1GT1BamHI-R	5'CGAGGATCC*GCCACCGTGATGGTGATGGTGATGGCCACC*ATTAT TTGTGTATTTTGTGA 3'	BamHI
P35	MYA1GT2XabI-F	5' CGATCTAGAATGCCAAGGACACCGCGGTCTGGT 3'	XbaI
P36	MYA1GT2BamHI-R	5' CGAGGATCC*GCCACCGTGATGGTGATGGTGATGGCCACC*ATCT GACCTTTCCAACAAGAA 3'	BamHI

P37	MYA1GT1BamHI-F	5’ CGAGGATCC*GGTGGCCATCACCATCACCATCACGGTGGC*CAGA AACAGCAGGAAAATCAA 3’	BamHI
P38	MYA1GT1NotI-R	5’ CGAGCGGCCGCTCAATTATTTTGTGTATTTTGTGA 3’	NotI
P39	MYA2GT2BamHI-F	5’ CGAGGATCC*GGTGGCCATCACCATCACCATCACGGTGGC*CCCAG ATCTTCTAAAGGAGGG 3’	BamHI
P40	MYA2GT2NotI-R	5’ CGAGCGGCCGCTCAGAATCTGAGCTTCTCAAC 3’	NotI
P41	MYA2GT1XbaI-F	5’ CGATCTAGAATGGAACGTCAAATTATGAATGTT 3’	XbaI
P42	MYA2GT1BamHI-R	5’ CGAGGATCC*GCCACCGTGATGGTGATGGTGATGGCCACC*AGAA TCTTTTCCAAAGGACCT 3’	BamHI
P43	XI-IGT2BamHI-F	5’ CGAGGATCC*GGTGGCCATCACCATCACCATCACGGTGGC*CCG AAAGCTTCACGAGGGATT 3’	BamHI
P44	XI-IGT2NotI-R	5’ CGAGCGGCCGCTCAAATGATCTGCTTTGAGGTTGA 3’	NotI
P45	XI-IGT1XbaI-F	5’ CGATCTAGAATGGAAAGAAACCTGGAGAACTAC 3’	XbaI
P46	XI-IGT2BamHI-R	5’ CGAGGATCC*GCCACCGTGATGGTGATGGTGATGGCCACC*AGAT TTTCCAGCAATCCCTCG 3’	BamHI
F47	XI-KGT2BamHI-F	5’ CGAGGATCC*GGTGGCCATCACCATCACCATCACGGTGGC*CCAAG GACATCAAGGGCAAGT 3’	BamHI
P48	XI-KGT2NotI-R	5’ CGAGCGGCCGCTTACGATGTACTGCCTTCTTT 3’	NotI
P49	XI-KGT1XbaI-F	5’ CGATCTAGAATGGAAAAGCAACAGGAAAACCAG 3’	XbaI
P50	XI-KGT1BamHI-R	5’ CGAGGATCC*GCCACCGTGATGGTGATGGTGATGGCCACC*AGC AACAGCATTTGCTTGTGC	BamHI
P51	Y1130A-F	5’ GCCTGTCTGATAGCCAAGTGTCTGATACAC 3'	
P52	R1137A-F	5’ CTGATACACTGGGCATCTTTTGAAGTAGAA 3'	
P53	P1514A-R	5’ GCAGTCGACTCATTCCAACAAGGCCATGAAGTTGGAGTTT TGGCG 3’	
P54	ΔE1517-R	5’ GCAGTCGACTCACAACAAGAACATGAAGTTGGA 3’	
P55	YCBamHI-R	5’ CGAGGATCCGTACAGCTCGTCCATGCCGAG 3’	BamHI
P56	MYA1CCBamHI-F	5’ CGAGGATCCGCTAGAAGAGAGCTTAGAATG 3’	BamHI
P57	YNXbaI-R	5’ CGATCTAGACATGATATAGACGTTGTGGCT 3’	XbaI
P58	YNBamHI-F	5’ CGAGGATCCATGGTGAGCAAGGGCGAGGAG	BamHI

Restriction enzyme site in each primer is underlined. The italic sequence encodes the linker GGHHHHHHGG in BiFC constructs or YFP tags.

Table S2: Summary of the plasmids constructed in this study

Plasmid name	Primers used	Expression Cassette	Utility
pACT-MYA1GT1	P1, P2	GAL4 AD::MYA1GT1(aa1099-aa1301)	Y2H
pAS1-MYA1GT2	P3, P4	GAL4 BD::MYA1GT2(aa1283-aa1520)	Y2H
pACT-MYA2GT1	P5, P6	GAL4 AD::MYA2GT1(aa1099-aa1297)	Y2H
pAS1-MYA2GT2	P7, P8	GAL4 BD::MYA2GT2(aa1279-aa1505)	Y2H
pACT-XIKGT1	P9, P10	GAL4 AD::XIKGT1(aa1124-aa1325)	Y2H
pAS1-XIKGT2	P11, P12	GAL4 BD::XIKGT2(aa1307-aa1545)	Y2H
pACT-XICGT1	P13, P14	GAL4 AD::XICGT1(aa1119-aa1320)	Y2H
pAS1-XICGT2	P15, P16	GAL4 BD::XICGT2(aa1302-aa1538)	Y2H
pACT-MYA1GT	P1, P4	GAL4 AD::MYA1GT(aa1099-aa1520)	Y2H
pAS1-MYA1GT	P17, P4	GAL4 BD::MYA1GT(aa1099-aa1520)	Y2H
pACT-MYA1GT1Δ1	P1, P18	GAL4 AD::MYA1GT1Δ1(aa1099-aa1263)	Y2H
pACT-MYA1GT1Δ2	P1, P19	GAL4 AD::MYA1GT1Δ2(aa1099-aa1279)	Y2H
pACT-MYA1GT1Δ3	P2, P20	GAL4 AD::MYA1GT1Δ3(aa1138-aa1301)	Y2H
pACT-MYA1GT1Δ4	P2, P21	GAL4 AD::MYA1GT1Δ4(aa1104-aa1301)	Y2H
pAS1-MYA1GT2Δ1	P3, P22	GAL4 BD::MYA1GT2Δ1(aa1283-aa1467)	Y2H
pAS1-MYA1GT2Δ2	P3, P23	GAL4 BD::MYA1GT2Δ2(aa1283-aa1485)	Y2H
pAS1-MYA1GT2Δ3	P3, P24	GAL4 BD::MYA1GT2Δ3(aa1283-aa1509)	Y2H
pAS1-MYA1GT2Δ4	P3, P25	GAL4 BD::MYA1GT2Δ4(aa1283-aa1513)	Y2H
pAS1-MYA1GT2Δ5	P3, P26	GAL4 BD::MYA1GT2Δ5(aa1283-aa1517)	Y2H
pAN-YN-MYA1GT2	P27, P28, P31, P32	YN(aa1-aa154)::MYA1GT2(aa1283-aa1520)	BiFC
pAN-MYA1GT1-YC	P29, P30, P33, P34	MYA1GT1(aa1099-aa1301)::YC(aa155-238)	BiFC
pAN-MYA1GT2-YC	P29, P30, P35, P36	MYA1GT2(aa1283-aa1520)::YC(aa155-238)	BiFC
pAN-YN-MYA1GT1	P27, P28, P37, P38	YN(aa1-aa154):: MYA1GT1(aa1099-aa1301)	BiFC
pAN-YN-MYA2GT2	P27, P28, P39, P40	YN(aa1-aa154)::MYA2GT2(aa1279-aa1505)	BiFC
pAN-MYA2GT1-YC	P29, P30, P41, P42	MYA2GT1(aa1099-aa1297)::YC(aa155-238)	BiFC
pAN-YN-XI-IGT2	P27, P28, P43, P44	YN(aa1-aa154):: XI-IGT2(aa1280-aa1522)	BiFC
pAN-XI-IGT1-YC	P29, P30, P45, P46	XI-IGT1(aa1115-aa1290)::YC(aa155-238)	BiFC
pAN-YN-XI-KGT2	P27, P28, P47, P48	YN(aa1-aa154):: XI-KGT2(aa1307-aa1545)	BiFC
pAN-XI-KGT1-YC	P29, P30, P49, P50	XI-KGT1(aa1124-aa1325)::YC(aa155-238)	BiFC
pACT-Y1130A	P1, P2, P51	GAL4 AD::MYA1GT1-Y1130A	Y2H
pACT- R1137A	P1, P2, P52	GAL4 AD::MYA1GT1-R1137A	Y2H
pACT-YRtoAA	P1, P2, P51, P52	GAL4 AD::MYA1GT1-Y1130A/R1137A	Y2H
pAS1- P1514A	P3, P4, P53	GAL4 BD::MYA1GT2-P1514A	Y2H
pAS1-ΔE1517	P3, P54	GAL4 BD::MYA1GT2Δ5-ΔE1517	Y2H
pAN-YFP-MYA1GT	P27, P32, P37, P55	YFP::MYA1GT(aa1099-aa1520)	FT
pAN-YFP-MYA1CCGT	P27, P32, P55, P56	YFP::MYA1CCGT(aa867-aa1520)	FT
pAN-YN-MYA1GT-YC	P27, P30, P33, P57	YN(aa1-aa154)::MYA1GT::YC(aa155-aa238)	BiFC
pAN-YFP-MYA1GT1	P27, P37, P38, P55	YFP::MYA1GT1(aa1099-aa1301)	FT
pAN-YFP-MYA1GT2	P27, P31, P32, P55	YFP::MYA1GT2(aa1283-aa1520)	FT
pAN-MYA2GT1-YFP	P30, P35, P36, P58	MYA2GT1(aa1099-aa1297)::YFP	FT
pAN-YFP-MYA2GT2	P27, P39, P40, P55	YFP::MYA2GT2(aa1279-aa1505)	FT

Y2H, yeast two-hybrid assay; BiFC, bimolecular fluorescence complementation; FT, fluorescence tagging.

SUPPLPEMENTARY DATA

The file MYA1_model.pdb contains the results from the Swiss-Model server. Included are the Myo2p template structure (PDB 2F6H) and the coordinates of the modeled MYA1 globular tail domain.

SUPPLEMENTARY FIGURE LEGENDS

Figure S1. **A** The structure model of MYA1 globular tail was evaluated to be biochemically robust by Ramachandran plot. 97.5% of all non-glycine residues within MYA1 globular tail fall into the energetically allowed regions in a Ramachandran map. The 10 non-glycine residues lying in the energetically unfavorable area in the Ramachandran map are labeled in black. Four proline residues that reside within or near the end of predicted helical region (P1093 in H1, P1123 in H3, P1245 and P1274 in H6) fall within the permitted range of Phi and Psi values (labeled in green). **B** Plot of the root-mean-square deviations (RMSD) of individual MYA1 amino acids relative to the structural template of Myo2p. Gaps in the alignment due to insertions or deletions between the two globular tail domains cannot be calculated and lead to negative RMSD values. Note that significant increases in RSMD values are always associated with these alignment gaps. Horizontal lines represent the predicted helical regions of MYA1 globular tail. Four proline residues residing in predicted helical regions are highlighted in green.

Figure S2. Protein gel blot analysis for point mutants that abolish Y2H interactions. To confirm that the GT1(Y1130A,R1137A) and GT2(F1514) point mutants could be expressed in yeast Y190 cells, a protein gel blot was used to detect the presence of the fusion proteins in the transformed cell lines. Recombinant proteins were detected with polyclonal antiserum raised against a combination of three MYA1-specific peptides. Lane 1: untransformed Y190 cells. Lane 2: cells expressing BD-GT2(F1514A) and AD-GT1. Lane 3: cells expressing BD-GT2 and AD-GT1(Y1130A,R1137A). Lane 4: cells expressing BD-GT2(F1514A) and AD-GT1(Y1130A,R1137A).

Figure S3. Alignment analysis of 12 *Arabidopsis* myosin XI tails and yeast myosin V (Myo2p) tail. The alignment was initially performed by MUSCLE and T-coffee algorithms and then manually optimized. AtXI-J was not included in the alignment since it lacks a globular tail. The corresponding α helices in myosin XI and myosin V were marked by purple and black bars, respectively. The conserved interacting triad within myosin XI globular tail is marked by arrow heads and the residues possibly involved in the motor-tail interaction of myosin V and XI are labeled by dots.

Figure S4. Localization of MYA1 globular tail subdomains with point mutations that disrupt GT1-GT2 interaction in plant cells. **A** YFP-GT1(Y1130A,R1137A) targeted to CFP-labeled peroxisome like the native form (see Fig. 5*A*). **B** YFP-GT2(F1514) targeted to CFP-labeled peroxisomes (compare to Fig. 5*B*).

Figure S1: (A) Ramachandran plot (B) RMSD values for individual amino acids in alignment

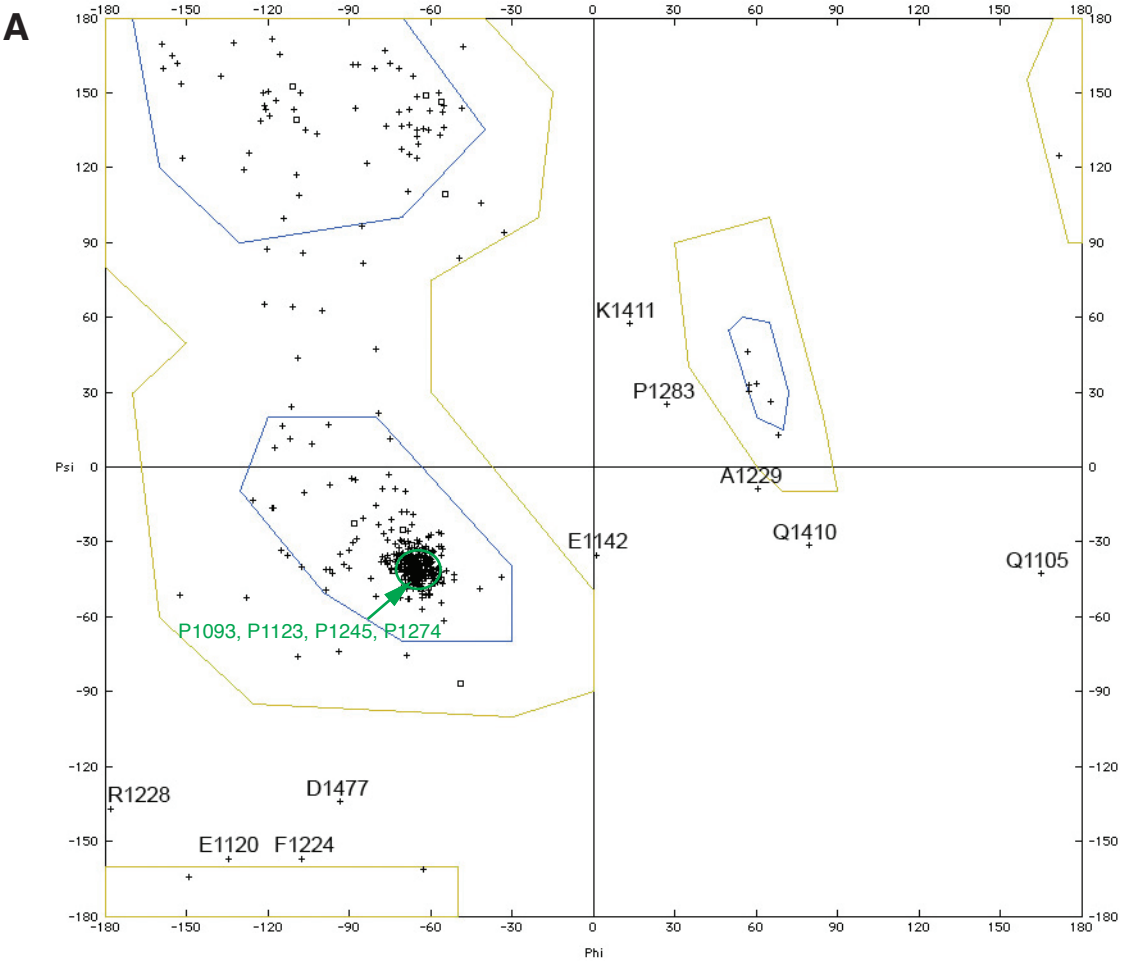

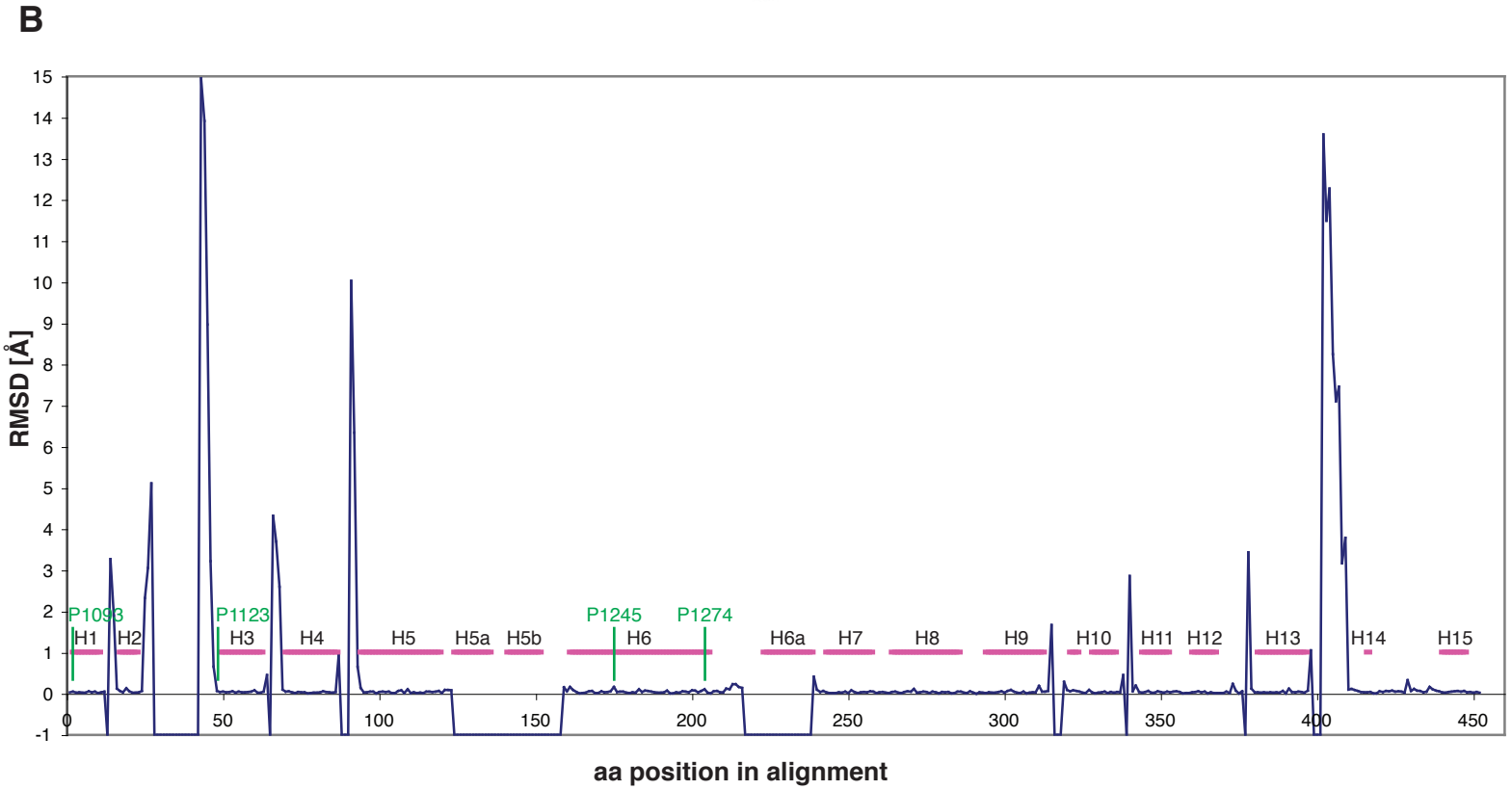

Figure S2: Expression of GT1 and GT2 point mutants in yeast cells

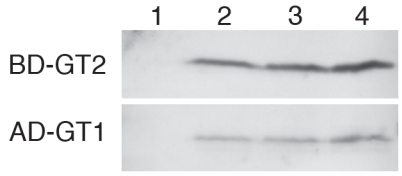

Figure S2: Alignment of Arabidopsis myosin XI globular tail sequences

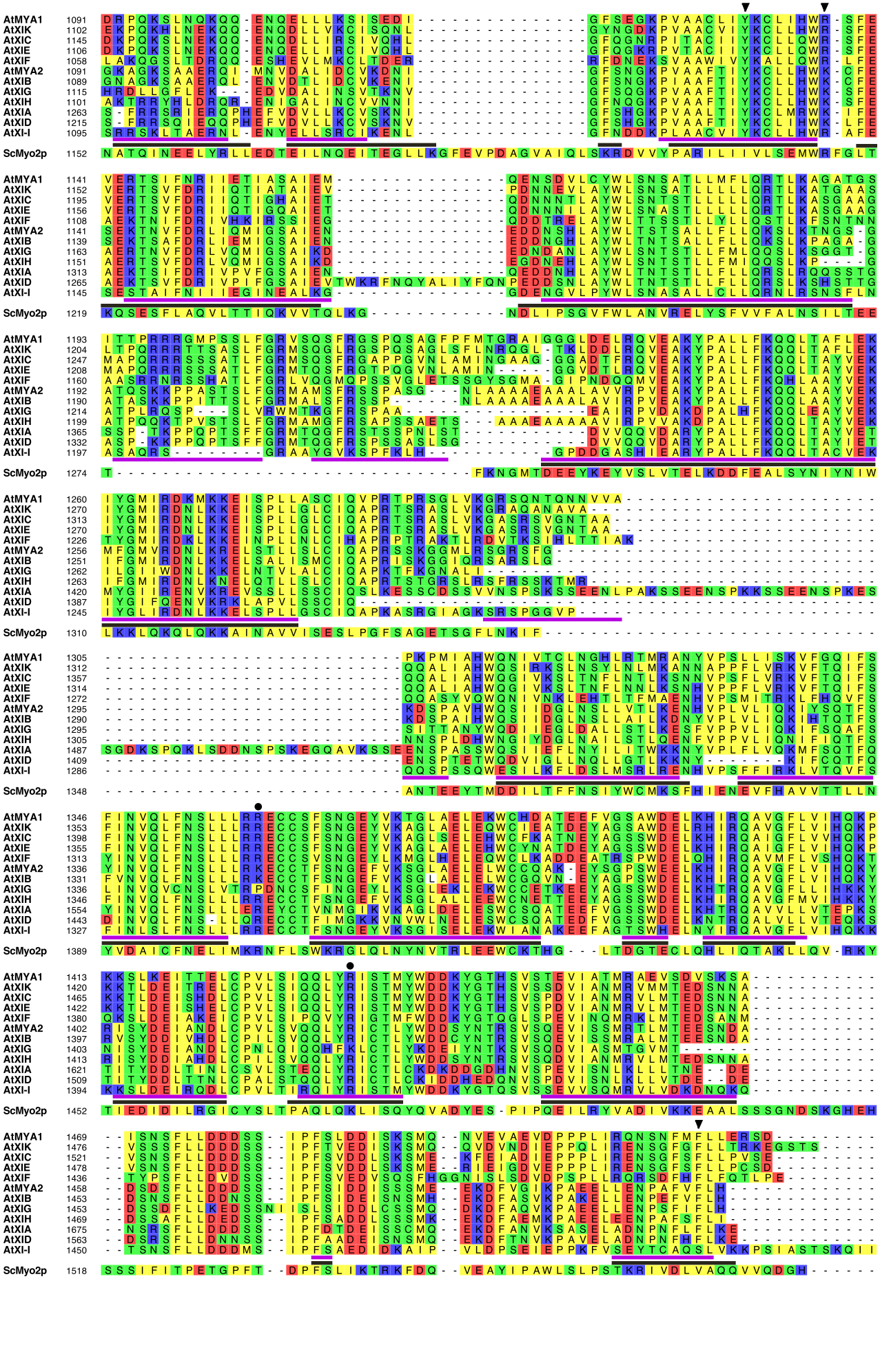

Figure S4: Localization of GT1 (A) and GT2 (B) point mutants